esting contrast. Both the width of the vibration and the absence of splittings make the H-H stretch similar to the D-D stretch of II. The solution to this problem must await further theoretical developments.

Acknowledgment. We thank Dr. M. Poliakoff for sharing ref 20 prior to its publication. Support for this work was provided by the donors of the Petroleum Research Fund, administered by the American Chemical Society, and by the Louisiana Quality Education Trust Fund, administered by the Louisiana Board of Regents. We also thank Michael DuQuesnay for his assistance with the synthesis of $M(CO)_5NH_3$.

Registry No. $Cr(CO)_5NH_3$, 15228-27-0; Ar, 7440-37-1; Xe, 7440-63-3; Kr, 7439-90-9; $Cr(CO)_5(H_2)$, 102286-49-7; D_2, 7782-39-0; H_2, 1333-74-0; $Cr(CO)_5$, 26319-33-5; $W(CO)_5NH_3$, 15133-64-9; $W(CO)_5(H_2)$, 102286-51-1; $Cr(CO)_5(HD)$, 102286-52-2; $Cr(CO)_5(D_2)$, 102286-55-5; $W(CO)_5(HD)$, 119907-64-1; $W(CO)_5(D_2)$, 117340-06-4.

Supplementary Material Available: A detailed description of the influence of ammonia on the spectrum of II, including two tables and two figures (13 pages). Ordering information is given on any current masthead page.

Electronic Structure Factors of Si-H Bond Activation by Transition Metals. The Valence Photoelectron Spectrum of $(\eta^5\text{-}C_5H_5)Mn(CO)_2HSiCl_3$

Dennis L. Lichtenberger* and Anjana Rai-Chaudhuri

Contribution from the Laboratory for Electron Spectroscopy and Surface Analysis, Department of Chemistry, University of Arizona, Tucson, Arizona 85721. *Received September 28, 1988*

Abstract: The valence photoelectron spectra of $HSiCl_3$ and $CpMn(CO)_2HSiCl_3$ (Cp = η^5-C_5H_5) have been obtained to provide a measure of the electronic structure factors that contribute to the interaction of the Si-H bond with a transition-metal center. The lowest valence ionizations of other $CpMn(CO)_2$(ligand) complexes are metal-based and reflect the formal d^6 electron count at the metal. The lowest valence ionizations in the He I photoelectron spectrum of $CpMn(CO)_2HSiCl_3$ are more stable and split over a wider energy range than has been observed previously. The chlorine lone pair based ionizations of $HSiCl_3$ coordinated to the metal have shifted about 1 eV to lower ionization energy from those of the free $HSiCl_3$ molecule. Both the stabilization of the metal-based ionizations and the destabilization of the ligand-based ionizations show that electron charge shift from the metal to the ligand more than compensates for the initial σ donation from the Si-H bond to the metal in $CpMn(CO)_2HSiCl_3$, as expected if the bonding has proceeded significantly toward oxidative addition. The relative intensity of the higher ionization energy component in the metal ionization region decreases with He II excitation, showing that this band is actually associated more with ligand character. This He I/He II relative intensity behavior corresponds to a formal d^4 electron count for the metal, consistent with the Mn(III) oxidation state. Fenske-Hall calculations indicate that the metal d hybrid orbitals available for the Mn-Si and Mn-H bonds form an acute angle between 50° and 70°, and these directed hybrids are responsible for the close proximity of the silicon and hydrogen atoms in the complex. These results are related to the other physical and chemical properties of this complex and are contrasted with the results of our similar photoelectron studies on the interaction of a carbon-hydrogen bond with the metal center in $(\eta^3\text{-}C_6H_9)Mn(CO)_3$, where the interaction primarily involves donation of C-H σ bonding orbital electron density into the empty metal orbitals in the formation of a 3-center 2-electron bond.

Knowledge of the factors controlling bond activation processes by transition metals is fundamental to understanding many important chemical reactions. The carbon-hydrogen bond is clearly one of the most desirable bonds to activate, and the interaction of the C-H bond with transition-metal centers has received much attention.[1-7] The general electronic factors of the bond activation process have been conveniently discussed in terms of a simple model in which there are two limiting descriptions of the electron distribution in the interaction.[8] In the early stages of the process σ activation is taking place, in which electron density from the C-H σ bond is donating into available empty metal levels to form a 3-center 2-electron bond. This interaction may be accompanied by competing filled-filled orbital interactions (i.e. steric repulsions) that will also play an important role in determining whether activation of the C-H bond will actually take place. For the C-H bond to be completely broken, the second stage of activation must take place in which electron density from filled metal levels donates into the empty C-H σ^* orbital, thereby completing the oxidative addition to formation of the alkyl metal hydride.

The electronic structure factors of C-H activation have been the subject of numerous theoretical investigations.[9-12] Photoelectron spectroscopy is able to provide direct experimental information on the strengths of individual bonding interactions with the metal center and the electron richness and charge potential throughout the complex.[13-15] An example is provided by the

* Author to whom correspondence should be addressed.

(1) Crabtree, R. H. *Chem. Rev.* **1985**, *85*, 245-269 and references therein.
(2) Crabtree, R. H. *Adv. Organomet. Chem.* **1988**, *28*, 299-338.
(3) Periana, R. A.; Bergman, R. G. *J. Am. Chem. Soc.* **1986**, *108*, 7346-7355.
(4) Buchanan, J. M.; Stryker, J. M.; Bergman, R. G. *J. Am. Chem. Soc.* **1986**, *108*, 1537-1550.
(5) Wenzel, T. T.; Bergman, R. G. *J. Am. Chem. Soc.* **1986**, *108*, 4856-4867.
(6) (a) Shilov, A. E. *Activation of Saturated Hydrocarbons by Transition Metal Complxes*; D. Riedal: Dordrecht, 1984. (b) Halpern, J. *Inorg. Chim. Acta* **1985**, *100*, 41-48.
(7) Jones, W. D.; Maguire, J. A. *Organometallics* **1986**, *5*, 590-591.
(8) Lichtenberger, Dennis L.; Kellogg, Glen Eugene *J. Am. Chem. Soc.* **1986**, *108*, 2560-2567.
(9) Saillard, J.-Y.; Hoffmann, R. *J. Am. Chem. Soc.* **1984**, *106*, 2006-2026.
(10) Obara, S.; Koga, N.; Morokuma, K. *J. Organomet. Chem.* **1984**, *270*, C33-C36.
(11) Eisenstein, O.; Jean, Y. *J. Am. Chem. Soc.* **1985**, *107*, 1177-1190.
(12) Shustorovich, E.; Baetzold, R. C.; Muetterties, E. L. *J. Phys. Chem.* **1983**, *87*, 1100-1113.

0002-7863/89/1511-3583$01.50/0

studies on (cyclohexenyl)manganese tricarbonyl, a molecule that displays an interaction of the C–H bond with the metal center as schematically shown in structure **1**.[16,17] Symmetry consid-

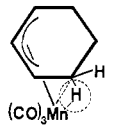

1

erations and theoretical calculations indicated that both the σ and σ^* activation modes might contribute to the stabilization of this complex in the observed geometry, but the calculations were unable to give a reliable quantitative indication of the relative importance of each mode.[8] The valence photoelectron (He I and He II) studies provided the information which showed that σ^* activation is relatively insignificant for this complex. A key observation was that the metal ionization band at 8.0 eV is not shifted or split as it would be by stabilization of one of the "t_{2g}" levels through delocalization to the C–H σ^* orbital.[8] The stabilization of the complex in its observed geometry derives from donation of the C–H bond electrons to low-lying empty metal levels to form a stabilized 3-center 2-electron bond. Unfortunately, direct observation of the stabilization of the ionization associated with the coordinated C–H bond is obscured by the ionizations of the other C–H bonds in organometallic complexes.[18]

Another important example of bond activation processes involves the interaction of a silicon–hydrogen bond with a transition-metal center. Transition-metal-assisted silane chemistry has significant practical consequences. Some of this chemistry, such as hydrosilation reactions, has received much attention. The Si–H studies are also valuable in assisting the understanding of C–H and other bond activation processes, because the qualitative features of C–H and Si–H bond activation are similar but specific quantitative contributions are much different. The key perturbations on the basic bonding scheme are the differences in the stability of σ and σ^* orbitals, the strengths of the bonds that are broken, the strengths of the bonds with the metal that are formed, the electronegativity of silicon in comparison to carbon, and the possibility of silicon d orbital participation. The inherently weaker Si–H bonds and correspondingly lower σ^* energies suggest that the Si–H bond should add to a given metal center more effectively than a normal C–H bond. Metal species that have weak interaction chemistry with C–H bonds may display strong interactions with certain Si–H bonds. The ability to tune the electron donation and acceptance abilities of the Si–H orbitals with substitutions on the silicon and the metal offers the possibility of characterizing stages of the bond breaking process from initial coordination to complete oxidation addition. Our results on the weak interaction of the C–H bond with the metal center in (cyclohexenyl)manganese tricarbonyl led naturally to our interest in transition-metal systems that display advanced stages of Si–H bond activation.

A series of compounds of the general formula $CpMn(CO)_2HSiR_3$ (where R is the substituent on silicon and Cp is η^5-C_5H_5) have been shown to exhibit Si–H bond activation. Graham and his co-workers first reported this remarkable class of complexes in 1971.[19,20] The special nature of these compounds has attracted much attention. Studies of the chemical and physical properties of these systems, most notably by Schubert,[21] Corriu,[22,23] and their co-workers, have greatly advanced the understanding of these systems. The complexes are generally obtained by the following reaction[19]

$$CpMn(CO)_3 + HSiR_3 \xrightarrow{h\nu} CpMn(CO)_2HSiR_3 + CO$$

This photochemical reaction scheme is typical for replacement of a carbonyl ligand in $CpMn(CO)_3$ by another 2-electron-donor ligand. The structures of the complexes appear as though the Si–H bond is occupying one of the coordination sites of the "piano-stool" complex, as illustrated below:

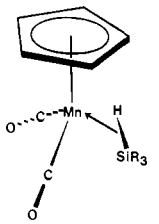

Graham first represented the bonding in terms of two possible canonical forms as shown by **2A** and **2B**.[19] Structure **2A** is a Mn^I,

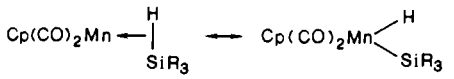

2A 2B

d^6 center with the Si–H bond behaving as a neutral 2-electron donor, consistent with other 2-electron-donor ligands to this $CpMn(CO)_2$ fragment. Structure **2B** represents oxidative addition to form a Mn^{III}, d^4 center with Mn–Si and Mn–H bonds in a seven-coordinate complex.

Numerous X-ray and neutron diffraction structural studies on this class of complexes have been reported by Schubert.[21] The Si–H bond lengths in these complexes are typically about 1.8 Å. For instance, the crystal structure of $MeCpMn(CO)_2HSiCl_3$ has been reported with a Si–H bond length of 1.79 Å.[24] This is longer than the Si–H covalent bond length of 1.48 Å but is shorter than the sum of the Van der Waal's radii of the two elements (3.1 Å). The bond distances suggest that the Si–H interaction in these Mn complexes is intermediate between a normal Si–H bond and a complete oxidative addition to the metal center.[21,24,25] However, the structures do not directly indicate the electronic features of charge distribution and bonding that result from the relative roles of the σ and σ^* interactions. Descriptions of the bonding and electron distribution derived from different experiments on these systems are not in complete agreement (see Discussion section).

Photoelectron spectroscopy is a unique tool for characterizing the bonding and electron distribution in transition-metal complexes. We report here the information provided by the valence ionizations of $CpMn(CO)_2HSiCl_3$. This molecule is particularly interesting because the chlorine lone pair ionizations provide a probe of the electron charge potential in the vicinity of the ligand, while the metal and Cp ionizations give a measure of the electron distribution and bonding of the ligand with the $CpMn(CO)_2$ fragment. We can compare our observations on this system with our results from previous studies on a large range of $CpMn(CO)_2L$ com-

(13) Lichtenberger, D. L.; Kellogg, Glen Eugene *Acc. Chem. Res.* **1987**, *20*, 379–387.
(14) Lichtenberger, Dennis L.; Kellogg, Glen Eugene; Pang, Louis S. K. In *Experimental Organometallic Chemistry*; Wayda, A. L., Darensbourg, M. Y., Eds.; American Chemical Society: Washington, DC, 1987; ACS Symp. Ser. 357.
(15) Lichtenberger, Dennis L.; Kellogg, Glen Eugene *Modern Inorganic Chemistry*; Russell, D. H., Ed.; 1987, in press.
(16) Brookhart, M.; Lamanna, W.; Humphrey, M. B. *J. Am. Chem. Soc.* **1982**, *104*, 2117–2126.
(17) Brookhart, M.; Green, M. L. H. *J. Organomet. Chem.* **1983**, *250*, 395–408.
(18) (a) Kellogg, G. E. *Diss. Abstr. Intl. B* **1986**, *46*, 3838. (b) Lichtenberger, D. L.; Kellogg, G. E.; Timmers, F.; Brookhart, M., to be submitted.
(19) Jetz, W.; Graham, W. A. G. *Inorg. Chem.* **1971**, *10*, 4–9.
(20) Hart-Davis, A. J.; Graham, W. A. G. *J. Am. Chem. Soc.* **1971**, *93*, 4388–4393.
(21) Schubert, U.; Scholz, G.; Muller, J.; Ackermann, K.; Worle, B. *J. Organomet. Chem.* **1986**, *306*, 303–326.
(22) Colomer, E.; Corriu, R. J. P.; Vioux, A. *Inorg. Chem.* **1979**, *18*, 695–700.
(23) Colomer, E.; Corriu, R. J. P.; Marzin, C.; Vioux, A. *Inorg. Chem.* **1982**, *21*, 368–373.
(24) Schubert, U.; Ackermann, K.; Kraft, G.; Worle, B. *Z. Naturforsch. B* **1983**, *38*, 1488–1492.
(25) Graham, W. A. G.; Bennett, M. J. *Chem. Eng. News* **1970**, *48* (*24*), 75.
(26) Hutcheon, W. L. Ph.D. Thesis, University of Alberta, Edmonton, 1971.

plexes.[13] The observations for the stage of activation demonstrated by the present Si–H bond interaction with the metal contrast significantly with the results of the early stages of C–H bond interaction with the metal,[8] and with the interpretations derived from other physical and theoretical studies of these metal–silyl systems.

Experimental Section

Preparation. $CpMn(CO)_2HSiCl_3$ was prepared by previously reported methods[19] and characterized by IR (in hexane and recorded on a Perkin-Elmer 983 spectrometer) and by proton NMR (in $CDCl_3$). The compound was carefully sublimed prior to introduction in the spectrometer and care was taken to see that it was free from any starting material. The compound sublimes cleanly as a pale yellow solid.

Photoelectron Data. Photoelectron spectra were recorded on an instrument that features a 36 cm radius hemispherical analyzer (10 cm gap), customized sample cells, excitation sources, detection and control electronics, and data collection methods that have been described previously.[18a,27-30] $CpMn(CO)_2HSiCl_3$ was run at a sample cell temperature of 50 °C for He I data collection and 52 °C for He II data collection. The spectrum of the compound was taken five times with no discernable difference between the spectra and no observable decomposition either before or after the compound sublimed. The data are represented analytically with the best fit of asymmetric Gaussian peaks (program GFIT).[31] The asymmetric Gaussian peaks are defined with the position, the amplitude, the half-width indicated by the high binding energy side of the peak (W_h), and the half-width indicated by the low binding energy side of the peak (W_l). The confidence limits of the peak positions (containing one or more peaks) and widths are generally ±0.02 eV. The confidence limit of the area of a band envelope is about ±5%, with uncertainties introduced in the baseline subtraction and fitting in the tails of the peaks. The individual areas of overlapping peaks are not independent and therefore are more uncertain.

Calculations. Orbital eigenvalues and characters were calculated by the Fenske–Hall method[32] for $CpMn(CO)_2HSiCl_3$. The atomic orbital functions and geometry of the $CpMn(CO)_2$ portion of the molecule were not changed from previous work.[33] The silicon functions were generated from Clementi's double-ζ functions for the neutral atom.[34a] The 3s functions were fit to single-ζ form and the 3p functions were fit to double-ζ form while maintaining Gram–Schmidt orthogonality to similarly constructed single-ζ core functions. A calculation was performed including the Si 3d orbitals but very little change in the basic orbital interaction was observed. The chlorine functions are Clementi's double-ζ core and triple-ζ valence functions without change.[34b] The Si–H bond distances and related angles were taken from the neutron diffraction structure of $MeCpMn(CO)_2HSiFPh_2$.[35] The Mn–Si and Si–Cl bond distances and related angles were taken from the X-ray structure of $MeCpMn(CO)_2HSiCl_3$.[24] The neutron diffraction structure of the molecule shows that the center of the coordinated Si–H bond is approximately on the binding site of the metal as defined by 90° angles with the two carbonyls. The 3-fold axis of the $SiCl_3$ group points within 2° of the metal according to the results of the crystal structure and is pointed directly at the metal in the calculations. The results of the calculation are transformed to the basis of the $CpMn(CO)_2$ fragment and the $HSiCl_3$ molecule in the coordinated geometry for clear representation of the orbital interactions. The calculations are also transformed to the basis of the $CpMn(CO)_2$ fragment and the $SiCl_3^-$ molecule in the coordinated geometry for a picture of the effects of protonation and deprotonation of the complex.

(27) Calabro, D. C.; Hubbard, J. L.; Blevins, C. H., II; Campbell, A. C.; Lichtenberger, D. L. *J. Am. Chem. Soc.* **1981**, *103*, 6839–6846.
(28) Lichtenberger, D. L.; Kellogg, G. E.; Kristofzski, J. G.; Page, D.; Turner, S.; Klinger, G.; Lorenzen, J. *Rev. Sci. Instrum.* **1986**, *57*, 2366.
(29) Lichtenberger, D. L.; Calabro, D. C.; Kellogg, G. E. *Organometallics* **1984**, *3*, 1623–1630.
(30) Hubbard, J. L. *Diss. Abstr. Intl. B* **1983**, *43*, 2203.
(31) Lichtenberger, D. L.; Fenske, R. F. *J. Am. Chem. Soc.* **1976**, *98*, 50–63.
(32) Hall, M. B.; Fenske, R. F. *Inorg. Chem.* **1972**, *11*, 768–775.
(33) Lichtenberger, D. L.; Sellmann, D.; Fenske, R. F. *J. Organomet. Chem.* **1976**, *117*, 253–264.
(34) (a) Clementi, E. *J. Chem. Phys.* **1964**, *40*, 1944–1945. (b) Clementi, E.; Roetti, C. *Atomic Data and Nuclear Data Tables* **1974**, *14*, 177–478.
(35) Schubert, U.; Ackermann, K.; Worle, B. *J. Am. Chem. Soc.* **1982**, *104*, 7378–7380.
(36) Schilling, B. E. R.; Hoffmann, R.; Lichtenberger, D. L. *J. Am. Chem. Soc.* **1979**, *101*, 585–591.
(37) Schilling, B. E. R.; Hoffmann, R.; Faller, J. W. *J. Am. Chem. Soc.* **1979**, *101*, 592–598.
(38) Lichtenberger, D. L.; Fenske, R. F. *Inorg. Chem.* **1976**, *15*, 2015–2022.

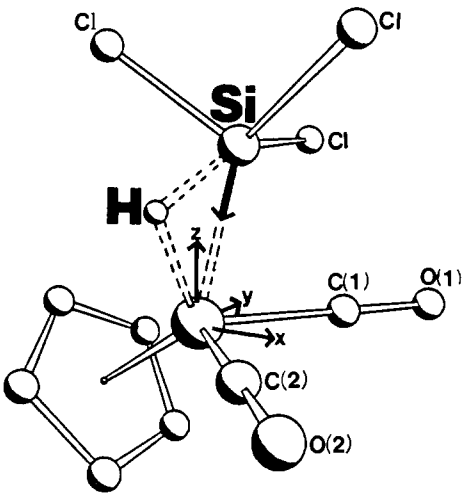

Figure 1. The coordinate system of $CpMn(CO)_2HSiCl_3$ used for the molecular orbital calculations.

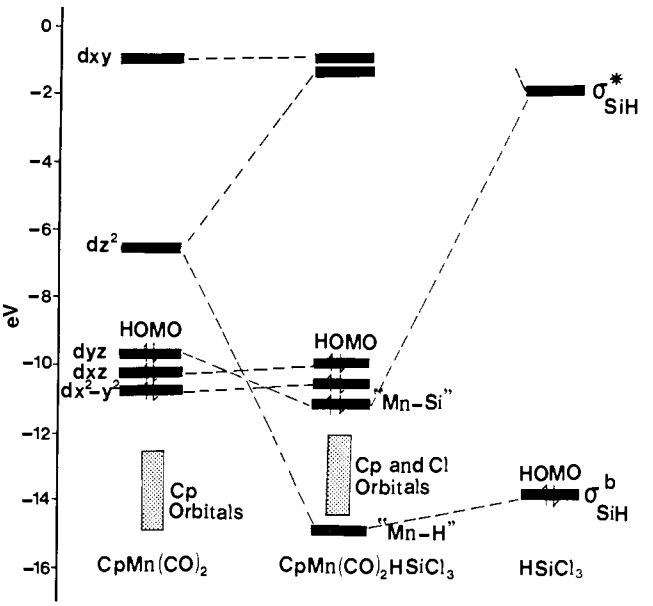

Figure 2. Molecular orbital diagram obtained by interacting $HSiCl_3$ with the $CpMn(CO)_2$ fragment.

Results

Orbital Interactions of $HSiCl_3$ with the $CpMn(CO)_2$ Fragment. Before presenting the information provided by the valence ionizations, it is useful to clarify the symmetry interactions that take place between $HSiCl_3$ and the $CpMn(CO)_2$ fragment and review the results of the Fenske–Hall calculations. The bonding capabilities of the $CpMn(CO)_2$ fragment have been described previously and applied to a large number of $CpMn(CO)_2L$ compounds, where L is commonly a two-electron-donor ligand like ammonia, phosphines, carbenes, alkenes, etc.[36-38] In this case the ligand L is $HSiCl_3$. $CpMn(CO)_2L$ compounds may be considered pseudo-octahedral if the cyclopentadienyl ring is viewed as occupying three coordination sites. The convenient coordinate system for describing the orbitals of $CpMn(CO)_2$ places the coordination site for ligand L along the z-axis, with the x-axis bisecting the two carbonyls. Figure 1 is a projection of the geometry of the molecule for the coordinate system for this discussion. The $CpMn(CO)_2$ fragment is able to coordinate many different kinds of ligand molecules partly because it possesses both donor and acceptor orbitals that are spatially and energetically favorable for bonding interactions. The LUMO of the $CpMn(CO)_2$ fragment is high in d_{z^2} character and directed along the bonding coordinate site. This orbital can accept two electrons from the ligand to form the M–L σ bond. The three highest occupied orbitals are principally metal d_{xz}, $d_{x^2-y^2}$, and d_{yz} in character. The orbital with d_{yz}

Table I. Molecular Orbital Characters

orbital	energy	character: metal	character: $HSiCl_3$ basis[a]	character: atomic basis
Mn d_{xz}	10.08	69% d_{xz}		
Mn $d_{x^2-y^2}$	10.67	54% $d_{x^2-y^2}$		
Mn–Si	11.21	36% d_{yz}	11% HOMO, 17% LUMO	8% Si, 0.4% H, 23% Cl
Mn–H	14.75	8% d_{yz}, 4% d_{z^2}	42% HOMO, 25% $SiCl_3$	2% Si, 9% H, 59% Cl

[a] In geometry of coordination.

Table II. Population Analysis

atomic charges: free $HSiCl_3$		atomic charges: metal complex		orbital populations: metal		$HSiCl_3$		CO[a]	
Si	1.14	Si	0.93	d_{xz}	1.58			$Co(1)2\pi_\perp$	0.38
Cl	−0.29	Cl	−0.29	$d_{x^2-y^2}$	1.37			$CO(1)2\pi_\parallel$	0.31
H	−0.26	H	−0.29	d_{yz}	1.28	LUMO	0.52	$Co(1)5\sigma$	1.46
		Mn	0.96	d_{z^2}	0.93	HOMO	1.76	$CO(2)2\pi_\perp$	0.28
				d_{xy}	0.89			$CO(2)2\pi_\parallel$	0.29
								$CO(2)5\sigma$	1.46

[a] 2π populations perpendicular and parallel to the $Mn(CO)_2$ plane.

character is the HOMO of the fragment and is well-situated for donation of π electron density to the ligand.

A molecular orbital diagram based on the results of the Fenske–Hall calculation is shown in Figure 2. The left side of the diagram shows the familiar orbitals of the $CpMn(CO)_2$ fragment. The right side of the diagram shows the calculated energy positions of the Si–H σ and σ^* orbitals. In the free $HSiCl_3$ molecule these Si–H orbitals are calculated to be in the same energy vicinity and strongly mixed with the other Si–Cl bonds and Cl lone pairs. This mixing is also evident in the photoelectron spectrum of free $HSiCl_3$ as discussed later. The longer Si–H distance in the coordinated geometry results in a clearer separation of the HOMO (containing Si–H σ) and the LUMO (containing Si–H σ^*) from the other orbitals, although considerable mixing still occurs. The energies of these orbitals of the distorted $HSiCl_3$ in the complex are shown in Figure 2 so that the remaining shifts represent the interacitons with $CpMn(CO)_2$.

Saillard et al. have extensively discussed the interactions of SiH_4 with the $CpMn(CO)_2$ fragment in terms of the results of extended Hückel calculations.[39] The extended Hückel and Fenske–Hall calculations agree in the qualitative orbital interactions. The primary characters of the molecular orbitals involving the Mn and Si–H interactions are summarized in Table I. As shown in the molecular orbital diagram and in Table I, the HOMO of the $CpMn(CO)_2$ fragment is high in d_{yz} character and has a strong interaction with the Si–H LUMO (σ^*) orbital. It is interesting to note that, as shown in the neutron diffraction measurements, the Si–H bond with its acceptor orbital aligns itself for interaction with the d_{yz}, which is the best π-donor orbital of the $CpMn(CO)_2$ fragment. The resultant molecular orbital is stabilized such that it becomes the third highest occupied orbital of the complex. The calculations show a net transfer of 0.52 electrons from the d_{yz} into the Si–H LUMO (σ^*) (Table II), which is greater than the calculated donation into a single carbonyl 2π orbital. Because of the substantial reduction in metal character of this orbital and the significant Si character, we give this orbital the label "Mn–Si" to denote the mixed metal and ligand character. This interaction will be important in the later discussion. The metal orbitals derived from the d_{xz} and $d_{x^2-y^2}$ are relatively unpertured by the interaction.

The Si–H HOMO (σ) orbital is interacting with the LUMO of the $CpMn(CO)_2$ fragment, and the calculations indicate a net stabilization of 1 eV in the resulting orbital in the complex. This molecular orbital is labeled "Mn–H" in Table I because of its predominant hydrogen character. The true nature of this orbital

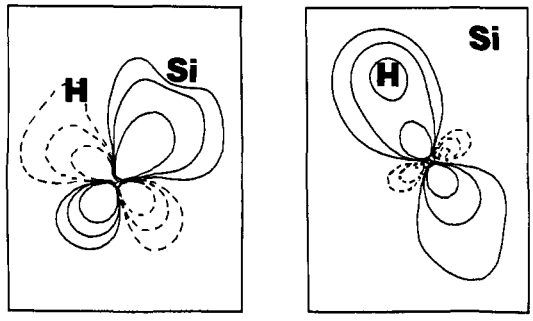

Figure 3. Calculated orbital contours for the "Mn–Si" and "Mn–H" orbitals. The contour values are 0.125, 0.0625, and 0.03125.

in the complex is important in determining if the bonding is best represented as 3-center 2-electron bonding or oxidative addition to Mn–H and Mn–Si σ bonds. A stabilization of about 1 eV is typical for two-electron-donor bonds to metals.[40,41] The population analysis (Table II) indicates that the donation is a little less than that of a carbonyl 5σ orbital. The donation of electron density from the Si–H σ bond, the acceptance of electron density into the Si–H σ^*, and the increased Si–H distance (1.8 Å) result in a calculated Si–H overlap population of 0.3 e^- in $CpMn(CO)_2HSiCl_3$ compared to 0.8 e^- for free $HSiCl_3$ (Si–H distance = 1.48 Å).

The discussion of the calculated results in terms of the Si–H σ and σ^* interactions with the metal can be misleading as to the extent that the resulting orbitals of the complex should be considered 3-center 2-electron bonds. This is because of the mixing among the orbitals of the silyl ligand referred to above. The effects of this mixing are shown in Table I where the primary orbital characters of the complex are listed in terms of the atoms of the $HSiCl_3$ ligand. In the orbital labeled "Mn–Si" there is primary ligand contribution from the Si–H σ^* (LUMO), but there is also significant contribution from the Si–H σ (HOMO). The combination of these contributions is such that it essentially cancels the contribution of the hydrogen atom to this orbital, and the orbital can be considered simply the directed Mn–Si σ bond. Likewise, the combination of the Si–H HOMO and the other $SiCl_3$ contributions to the orbital labeled "Mn–H" in the complex largely cancels the silicon contribution to this orbital, and the orbital is simply the primary contribution to the Mn–H σ bond (considerable mixing with the chlorine lone pairs remains because of their close energy proximity). Thus both of these orbitals appear more as directed Mn–H and Mn–Si σ bonds than as 3-center 2-electron bonds.

The contours of the "Mn–Si" and "Mn–H" orbitals are illustrated in Figure 3. The orbital labeled "Mn–Si" appears to be primarily the Mn–Si bond formed from a hybrid of the metal d_{z^2} and d_{yz} (mostly d_{yz}) orbitals such that the metal orbital is directed at the Si atom. The H atom is positioned near the node of this orbital and has little contribution. The orbital labeled "Mn–H" is largely the Mn–H bond and is formed from the other hybrid of the d_{z^2} and d_{yz} (mostly d_{z^2}) orbitals such that the metal orbital is directed at the H atom. There is very little contribution of the Si atom in this orbital. The importance of these metal hybrids will be discussed later.

The charge analysis in Table II shows that the Si and H atoms are calculated to accept a small amount of negative charge when coordinated to the metal. This is in contrast to the extended Hückel results[39] that predicted a net loss of electron density from SiH_4 when coordinated to the metal. These results were interpreted as a dominance of the 3-center 2-electron bond formation and less contribution from the Si–H σ^* orbital. Thus the extended Hückel and Fenske–Hall calculations are not in agreement as to the extent that the addition has proceeded to the formation of

(39) Rabaa, H.; Saillard, J.-Y.; Schubert, U. *J. Organomet. Chem.* **1987**, *330*, 397–413.

(40) Lichtenberger, D. L.; Kellogg, G. E.; Landis, G. H. *J. Chem. Phys.* **1985**, *83*, 2759–2768.

(41) Bursten, B. E.; Darensbourg, D. J.; Kellogg, G. E.; Lichtenberger, D. L. *Inorg. Chem.* **1984**, *23*, 4361–4365.

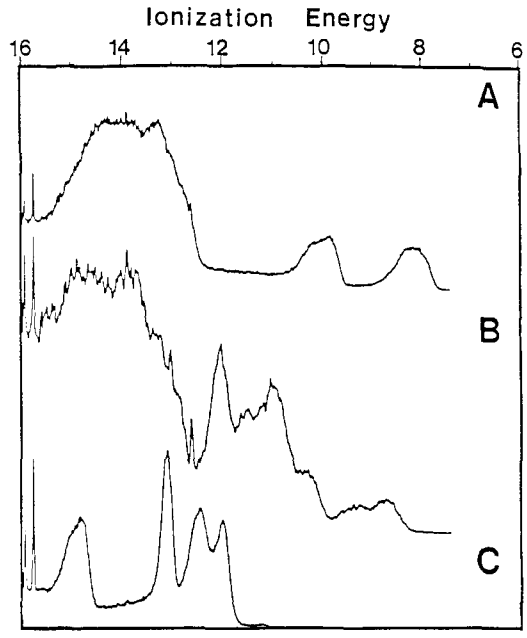

Figure 4. Comparison of the He I photoelectron spectra of (A) $CpMn(CO)_3$, (B) $CpMn(CO)_2HSiCl_3$, and (C) $HSiCl_3$.

distinct Mn–H and Mn–Si σ bonds, with formal H^- and $SiCl_3^-$ ligands, and a formal d^4 Mn(III) center.

We wish to emphasize that the summary of the Fenske–Hall results presented in this section is for the purpose of introducing the basic electronic interactions. Comparison with the extended Hückel results illustrates differences in the relative contributions of these interactions according to different theoretical models. The calculations were not done for the purpose of assigning the valence ionizations. The limitations of Koopmans' theorem, electron correlation, and calculational models for assigning ionizations are well-known.[13] The observed features of the ionizations presented in the next section provide the experimental information for the actual electron distribution, formal oxidation state, and nature of the bonds in the $CpMn(CO)_2HSiCl_3$ molecule. As will be seen, the order and nature of the ionizations as determined by these experiments is generally the same as obtained from the Fenske–Hall calculations.

Valence Ionization Bands and Assignments. The He I valence photoelectron spectrum of $CpMn(CO)_2HSiCl_3$ from 6 to 16 eV ionization energy is shown in Figure 4. The assignment of the valence ionizations of this complex is aided by comparison to the ionizations of the free $HSiCl_3$ molecule and $CpMn(CO)_3$, which are also shown in Figure 4. The spectra of both $CpMn(CO)_2HSiCl_3$ and $CpMn(CO)_3$ show a broad band of overlapping ionizations from about 12–16 eV ionization energy. The ionizations expected to occur in this region are associated with the carbonyl 5σ and 1π orbitals and the Cp a_2'' (symmetric π) and valence σ orbitals. Individual assignments in this forest of ionizations will not be attempted.

Before focusing on the detailed features of the ionizations in the low valence region, it is helpful to examine the ionizations of the free $HSiCl_3$ molecule. An assignment of the valence ionizations of the $HSiCl_3$ molecule has been reported previously,[42] but some of the ionizations were conjectured to be accidentally degenerate and were not separately observed. Our closeup photoelectron spectrum of $HSiCl_3$ is shown in Figure 5. The ionizations of $HSiCl_3$ in the region from 12–13 eV are due primarily to the ionizations of the Cl lone pairs, as is similarly observed in the photoelectron spectrum of $SiCl_4$.[43] The six chlorine ($p\pi$) lone pairs form symmetry combinations that are comprised of the a_2, a_1, and two e sets. According to Frost et al., the a_2 combination

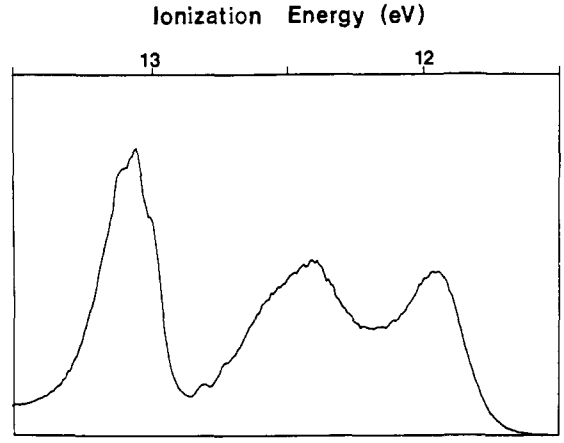

Figure 5. Closeup He I photoelectron spectrum of $HSiCl_3$.

Table III. He I Valence Ionization Features

	position	W_h	W_1	relative area
$CpMn(CO)_2HSiCl_3$				
M	8.69	0.55	0.51	1.00
ML	9.32	0.55	0.51	0.59
Cp	10.27	0.59	0.34	1.33
	10.66	0.59	0.34	0.79
A	10.95	0.33	0.41	2.40
B	11.23	0.33	0.41	2.01
C	11.59	0.33	0.41	2.30
D	12.04	0.46	0.37	4.39
$HSiCl_3$				
A	11.95	0.37	0.21	0.73
B	12.39	0.32	0.33	0.72
C	12.62	0.32	0.33	0.37
D	13.07	0.28	0.18	1.00

is assigned to the ionization at 11.94 eV, the e and a_1 combinations are assumed degenerate at 12.41 eV, and the second e combination is assigned to the ionization at 13.07 eV. These reported positions are in excellent agreement with our results for band A (11.95 eV), band B (12.39 eV), and band D (13.07 eV) shown in Table III. In addition, we observe a shoulder on the high binding energy side of the second ionization band at about 12.6 eV which we label band C (see Figure 5). Observation of this shoulder supports the proposal of Frost et al. of the near degeneracy of the first e and the a_1 ionizations in this band. Vibrational fine structure is observable on the high binding energy side of this band as well as on several of the other bands. Detailed assignment of the vibrational modes is not attempted in this work. The ionizations in the range of 14–15 eV correspond to the Si–Cl σ bonds. The previous investigators assigned the Si–H ionization to the high binding energy side of the Si–Cl σ ionizations at 14.8 eV. This position of the Si–H ionization is also consistent with Fenske–Hall calculations on $HSiCl_3$. The close energy proximity of the Si–H ionization to the other ionizations of similar a_1 symmetry means that there is substantial mixing between these orbitals, and one cannot talk about a single a_1 ionization as representing all of the Si–H bonding.

The valence ionization features of $CpMn(CO)_2HSiCl_3$ from 8 to 13 eV (He I and He II) are shown in Figure 6. The relative intensity pattern and splitting of the chlorine lone pair ionizations observed in the spectrum of the free $HSiCl_3$ molecule is also observed in the He I ionizations of $CpMn(CO)_2HSiCl_3$, but shifted about 1 eV to lower binding energy. The shift to lower ionization energy is indicative of greater negative charge potential in the region of $SiCl_3$ when $HSiCl_3$ is coordinated to the metal. The change in appearance of the B and C ionizations of $CpMn(CO)_2HSiCl_3$ compared to the more nearly degenerate **B** and C ionizations of free $HSiCl_3$ is additional proof that at least two different ion states occur in this region. One of these ionizations is a_1 symmetry and likely contains some of the Si–H interaction, and it is reasonable that this region of the ionizations shows the most perturbation when the Si–H bond coordinates to the metal.

(42) Frost, D. C.; Herring, F. G.; Katrib, A.; Mclean, A. N.; Drake, J. E.; Westwood, N. P. C. *Can. J. Chem.* **1971**, *49* (24), 4033–46.
(43) Green, J. C.; Green, M. L. H.; Joachim, P. J.; Orchard, A. F.; Turner, D. W. *Phil. Trans. R. Soc. London A* **1970**, *268*, 111–130.

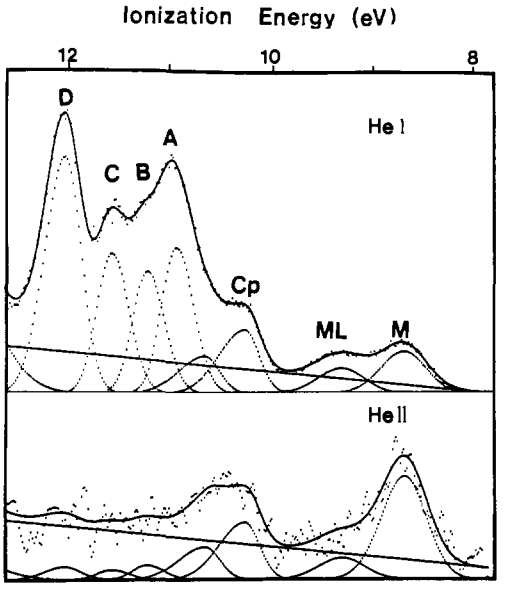

Figure 6. He I/He II comparison of the valence ionizations of $CpMn(CO)_2HSiCl_3$.

The band at ≈10.3 eV correlates with the Cp e_1'' predominantly ring π ionizations and is labeled Cp in Table III. The Cp ionization in the spectrum of $CpMn(CO)_3$ and in the spectra of a large number of other $CpMn(CO)_2L$ complexes[27] has a characteristic shoulder on the high binding energy side. In the spectrum of $CpMn(CO)_2HSiCl_3$, this Cp ionization occurs on the low binding energy side of the ionization bands due to the Cl lone pairs and the Cp ionization shoulder is not clearly observed. However, it is necessary to include the shoulder on the Cp ionization in the analytical representation of the spectrum of $CpMn(CO)_2HSiCl_3$, otherwise, the chlorine lone pair ionization A becomes unrealistically skewed to low binding energy.[44] The Cp ionization shoulder is constrained to have the same splitting and relative intensity as was observed in the spectrum of $CpMn(CO)_3$. Independent of the analytical representation of the band, the Cp ionization in $CpMn(CO)_2HSiCl_3$ is shifted to higher binding energy (0.4 eV) compared to its position in $CpMn(CO)_3$. The Cp e_1'' is donating to empty metal levels, and the shift to higher binding energy is indicative of a more positive metal center in the complex.

In the spectrum of $CpMn(CO)_3$, the ionization at about 8 eV represents the predominantly metal levels of the d^6 complex. The observation of a single band in this region follows from the near degeneracy of the "t_{2g}" levels of the pseudo-octahedral complex. In the spectrum of $CpMn(CO)_2HSiCl_3$, a pair of partially resolved peaks with an intensity pattern of approximately 2:1 (low-energy component to high-energy component) is observed in this region (see Figure 6 and Table III). The leading ionization band in $CpMn(CO)_2HSiCl_3$ occurs at 0.7 eV higher binding energy than the metal band in $CpMn(CO)_3$. One of the ionizations in this region represents a metal orbital that is primarily backbonding to the carbonyls and has little interaction with the $HSiCl_3$ group. Like the shift of the Cp ionization, the shift of this ionization to higher ionization energy is a measure of increasing positive charge potential at the metal center. This is discussed in greater detail later.

Figure 6 also shows the He I/He II comparison of the 8–13 eV region of $CpMn(CO)_2HSiCl_3$. The He I/He II intensity trends provide additional evidence for the assignment and interpretation of all of the ionizations. The He II photoelectron spectrum has been represented with peaks at the same positions and with the same high-energy and low-energy half-widths as in the He I data. Only the peak amplitudes are allowed to vary between the representations of the He I and He II data. This procedure is appropriate because the positions and widths are determined best in the higher signal-to-noise He I data, and only the amplitudes are different in the He II spectrum because of the energy dependence of the cross-sections. The bands due to the Si–Cl and Cl lone pair electrons (12.5–10.6 eV) show negligible intensity in the He II spectrum. This is expected because of the relatively low He II photon cross-sections of the Cl orbitals.[45] Theoretical calculations of the relative cross-sections illustrate the basic trends.[46] The Cl 3p photoionization cross-section falls by a factor of 20, while carbon falls by a factor of 3 on going from He I to He II. Consequently, the Cp ionization band gains intensity relative to the Cl lone pair ionizations in the He II spectrum.

The manganese 3d photoelectron cross-section is calculated to increase from He I to He II excitation, and the first ionization band (band M) grows substantially in intensity in He II relative to any other ionizations. The relative intensity of the metal-based to Cp-based ionizations is well-known from the spectrum of $CpMn(CO)_3$, and comparison with the relative intensity of the M and Cp ionizations observed here shows that the intensity of band M corresponds to four metal-based electrons relative to the four Cp-based electrons.

The ionization band at 9.3 eV would normally be considered to account for the additional two metal electrons. However, the 0.6-eV stabilization of this ionization relative to the other metal-based ionizations is quite large for $CpMn(CO)_2L$ type of complexes. Furthermore, the ionization at 9.3 eV shows relatively little growth from He I to He II excitation and must be ligand based. Because of this behavior, we label this ionization ML for further discussion. The significance of these observations will be explained in detail in the next section.

Discussion

Nearly all of the references to the chemistry and properties of $CpMn(CO)_2HSiCl_3$ have addressed the question of the bonding and electron distribution resulting from Si–H interaction with the metal center. Some of the observations in these studies have been interpreted as evidence for retention of Si–H interaction in the complex, while others have suggested the molecule behaves like a full oxidative addition product. Retention of Si–H interaction in the complex involves formation of a 3-center 2-electron Mn–H–Si bond from donation of the Si–H σ bonding electron density to empty metal levels. Donation from the metal to the Si–H σ^* orbital is not sufficient to completely break the Si–H bond, and the metal retains a formal d^6 configuration in this kind of complex.[39] Complete oxidative addition involves formation of direct Mn–Si and Mn–H bonds from the metal interaction with the Si–H σ and σ^* orbitals. This results in substantial charge transfer to the $SiCl_3$ and H ligands and creation of a formal d^4 configuration for the metal. The ionizations of $CpMn(CO)_2HSiCl_3$ reported in the previous section show this complex to be a nearly complete oxidative addition product. These conclusions will be examined in detail first. We will then focus on a more complete picture of the interactions that are taking place in this molecule. Finally, we will show that the picture that emerges from these studies helps in understanding the other physical properties and the chemical behavior of this complex.

Ionization Information. There are several indications from the information in the ionizations of substantial electron charge shift from the metal to silicon and formation of a formally d^4 Mn^{III} center. For one, the shift of the chlorine lone pair ionizations gives a good indication of the charge redistribution toward the $SiCl_3$ portion of the molecule. The $SiCl_3$ ligand ionization bands (largely the Cl lone pairs) in $CpMn(CO)_2HSiCl_3$ are shifted 1 eV to lower binding energy compared to the corresponding ionizations of the free trichlorosilane molecule. This destabilization of the ligand-based levels follows from extensive negative charge delocalization to silicon, as would be expected with oxidative addition. In fact, the Cl lone pair ionizations appear in the same energy vicinity as the Cl lone pair ionizations in the photoelectron

(44) Lichtenberger, D. L.; Copenhaver, A. S.; Gray, H. B.; Marshall, J. L.; Hopkins, M. D. *Inorg. Chem.*, in press.

(45) Didziulis, S. V.; Cohen, S. L.; Butcher, K. D.; Solomon, E. I. *Inorg. Chem.* **1988**, *27*, 2238–2250.

(46) Yeh, J. J.; Lindau, I. *Atomic Data and Nuclear Data Tables* **1985**, *32*, 7–14.

spectrum of $CpFe(CO)_2SiCl_3$, where a direct Fe–Si bond exists[47] and the $SiCl_3$ group has a formal −1 charge.

A simple point charge-potential model[48] analysis of the shift of the chlorine lone pair ionizations gives a first approximation to the amount of charge transferred from the metal to silicon. The contribution to the shift from the amount of electron charge δ transferred from the metal to silicon is given by the equation

$$\Delta IP_{Cl} = \delta/R_{Mn-Cl} - \delta/R_{Si-Cl}$$

The negative sign for the increased δ charge on the silicon center means that the IP shifts to lower ionization energy. The R_{Mn-Cl} and R_{Si-Cl} distances were obtained from the crystal structure data of $MeCpMn(CO)_2HSiCl_3$.[24] This analysis shows that a 1-eV shift of the Cl lone pair ionizations implies a transfer of at least a 0.3-electron charge from the Mn center to the Si center. If the Mn center is more realistically assumed to have a partial positive charge, the shift of charge from the metal toward silicon must be even greater to offset the stabilization of the lone pair ionizations that occurs from bringing them into the region of positive charge potential. If the metal has an initial effective positive charge potential of 0.5 electron, then the shift of charge from the metal to silicon is 0.9 electron. Of course, this model is very approximate, as is any evaluation and discussion of atomic charge in a molecule. The point of this example is to emphasize that the chlorine lone pair ionizations are sensitive to electron charge shifts toward silicon, and will shift even if the charge on the chlorines themselves does not change.

The band on the low binding energy side of the chlorine lone pair ionizations at ≈10.3 eV is attributed to the presence of the Cp e_1'' orbitals. This ionization is shifted to higher binding energy compared to the Cp ionizations in $CpMn(CO)_3$. The filled Cp e_1'' levels are involved in donation to empty metal levels to form the primary bonding between the ring and the metal.[8,27,31] The shift of this ionization to higher binding energy denotes a more positively charged metal center (point charge stabilization as discussed above) as well as a less negative charge on the ring from more effective donation into the stabilized empty metal levels of $CpMn(CO)_2HSiCl_3$.

The first ionization band of the complex is predominantly metal in character and is shifted 0.7 eV to higher binding energy compared to the metal band in $CpMn(CO)_3$. This shift also indicates a stabilization of the metal orbitals as would be expected with a higher positive charge at the metal center. Thus we have the interesting situation of destabilization of the $SiCl_3$-based ionizations and stabilization of metal-based and Cp-based ionizations. This is further support of an electron distribution tending toward oxidative addition to give a Mn^{III} species.

The peak at 9.3 eV is a ligand-based ionization as obtained from the He I/He II intensity trends. It is also shifted substantially to higher binding energy from the metal-based ionization M than is normally observed if it retained major metal character. The decrease in relative intensity in He II is more consistent with silicon character than with hydrogen character. Because this ionization is ligand-based, this leaves the formal electron count at the metal at d^4 (from band M), corresponding to the Mn^{III} oxidation state. This is one of the most significant observations from the photoelectron data. In terms of the Si–H σ and σ^* description of the bonding, it means that the σ^* orbital is extensively involved in withdrawing electron density from the metal center.

A stepwise correlation diagram of ionization energies in the metal region helps in the understanding of the splitting pattern of the metal-based levels in $CpMn(CO)_2HSiCl_3$, particularly the degeneracy of two orbitals observed in the leading ionization band (see Figure 6). Figure 7 is a schematic diagram showing the stabilization/destabilization of the metal-based ionizations in a series of steps from $CpMn(CO)_3$ to $CpMn(CO)_2HSiCl_3$. The first column shows the measured energies of the metal-based ionizations of $CpMn(CO)_3$. These represent the e and the a symmetry combinations of the $Mn(CO)_3^+$ fragment as discussed previously.[49]

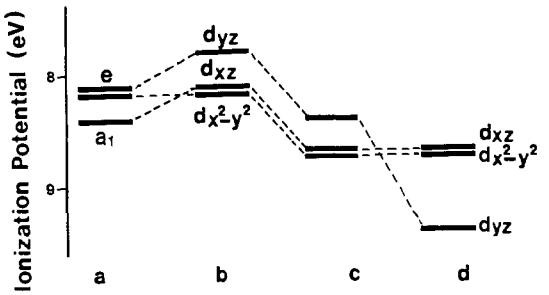

Figure 7. Stepwise correlation of experimental ionization energies: (a) $CpMn(CO)_3$ (observed); (b) $CpMn(CO)_3$ without overlap interaction of axial CO π^*; (c) $CpMn(CO)_2HSiCl_3$ without overlap interaction of Si–H σ^*; (d) $CpMn(CO)_2HSiCl_3$ (observed).

The second column shows the loss of π back-bonding stabilization from a carbonyl along the z axis (without redistribution of charge). The figure shows the primary metal orbital contributions in this coordinate system with ligand substitution on the z axis. This loss of π back-bonding to the z-axis ligand results in destabilization of the metal d_{xz} and d_{yz} orbitals of about 0.3 eV as determined from the spectra of $CpMn(CO)_2L$ complexes where L has no π back-bonding capability.[18a,40,41] The $d_{x^2-y^2}$ orbital, which does not overlap with ligand orbitals on the z axis, remains at the same energy. This 0.3-eV shift of the d_{xz} and d_{yz} orbitals produces a 1:2 splitting pattern of the metal-based ionizations. The third column shows the $HSiCl_3$ ligand in the final geometry and charge distribution with the $CpMn(CO)_2$ fragment but does not include the effects of orbital overlap. The difference in charge potential at the metal when the ligand is silane in comparison to carbonyl is reflected in the shift of the $d_{x^2-y^2}$ ionization. All three d orbitals are stabilized equally due to the higher positive charge at the metal center. The final stage in our stepwise approach completes the actual orbital overlap interaction of $HSiCl_3$ with the $CpMn(CO)_2$ fragment orbitals. The d_{yz} orbital interacts strongly with the Si–H σ^* orbital. The d_{yz} orbital does not remain a simple back-bonding orbital but forms the delocalized Mn–H–Si ionization as discussed below. The $d_{x^2-y^2}$ and d_{xz} orbitals do not interact with the silane and remain close together in energy, thus reproducing the intensity pattern observed in the photoelectron spectrum.

Formation of Mn–Si and Mn–H Bonds. Saillard et al. have modeled the orbital interactions that take place in these systems with extended Hückel calculations on $CpMn(CO)_2HSiH_3$.[39] The order of the frontier symmetry orbitals found in the extended Hückel calculation is the same as the order of the valence ionizations. However, the description of the electronic structure and bonding is considerably different from that obtained from the experiment. The extended Hückel calculations emphasize the weakening of the Si–H bond through the symmetric interaction corresponding to delocalization of the Si–H σ bonding pair toward the Mn atom (leaving 1.63 electrons in the Si–H σ bond by the extended Hückel calculations). The antisymmetric interaction corresponding to the delocalization of a metal π symmetry orbital into the Si–H antibonding σ^* orbital is considered to be less significant by the extended Hückel calculations (a charge transfer of 0.39 electron). The overall result of the extended Hückel calculations is that the SiH_3 group is actually left with a partial positive charge and is denoted as SiH_3^+. The σ interaction is calculated to be the predominant electronic mechanism taking place. This is in direct contradiction to the observations from the valence ionizations, which indicate a substantial occupation of the σ^* and a charge shift toward the silicon to make a formally −1 charged $SiCl_3$ unit.

The Fenske-Hall calculations agree with the extended Hückel calculations and the information from the valence ionizations as to the qualitative orbital interactions and the order of the low valence ionizations. The significant difference between the Fenske–Hall calculations and the extended Hückel calculations

(47) Lichtenberger, D. L.; Rai-Chaudhuri, Anjana, in preparation.
(48) Jolly, W. L.; Perry, W. B. *Inorg. Chem.* **1974**, *13*, 2686–2692.
(49) Lichtenberger, D. L. *Diss. Abstr. Intl. B* **1975**, *35*, 4856.
(50) Lichtenberger, D. L.; Darsey, G. P.; Kellogg, G. E.; Sanner, R. D.; Young, V. G.; Clark, J. R. *J. Am. Chem. Soc.*, submitted for publication.

is the greater extent of charge delocalization from the metal to silicon in the Fenske–Hall results. The Fenske–Hall calculations indicate a stronger back-bonding to the Si–H σ^* orbital and a slight net negative charge for the $HSiCl_3$ ligand as a whole. As described in the results section and most clearly illustrated in Figure 3, the orbital labeled "Mn–Si" that results from the interaction becomes a directed Mn–Si bond from the d_{yz} orbital hybridized with the d_{z^2}. The hydrogen atom is near the node of the orbital and contributes very little. Likewise, the orbital originating primarily from the Si–H σ bond actually becomes the directed Mn–H bond formed from the d_{z^2} orbital hybridized with the d_{yz}. This orbital contains very little Si character.

Even though the Fenske–Hall calculations point to directed Mn–Si and Mn–H bonds, the charge shift to the $SiCl_3$ ligand given by the calculations is not as great as the charge shift indicated by the ionizations. The calculations give an increase of 0.2 electron on the silicon atom in the complex compared to the silicon atom in $HSiCl_3$. The most telling feature is the shift of the chlorine lone pair ionizations with coordination of the ligand to the metal. The calculations show a shift of only 0.7 eV, compared to the 1-eV shift that is observed. This indicates that the calculations most likely underestimate the extent of oxidative addition to the metal. The cause for the underestimation of charge redistribution may be due to a number of factors in these calculations. We investigated the inclusion of silicon d orbitals on the calculated results. Although the silicon d orbitals were involved in π back-bonding from the chlorines to the silicon, they had little effect on the interactions with the metal.

Mn–Si bond ionization energies have been reported at 9–10 eV in the photoelectron spectra of $R_3SiMn(CO)_5$ complexes,[51] which is in good agreement with the 9.3-eV ML ionization observed in this complex. The Mn–H bond ionization energy in $Mn(CO)_5H$ is at 10.5 eV.[51] The reasonably close energy proximity of these two ionizations means that mixing is possible. The mixing of M–H and M–L bonds has been observed in the spectra of other complexes[50] although this does not seem to take place in $CpMn(CO)_2HSiCl_3$. The indication from the calculations is that, even though the electron density of these two bonds is spatially crowded in this complex, the hydrogen atom is near the node of the Mn–Si bond and the mixing is small (Figure 3). From these considerations and the He I/He II intensity behavior we conclude that the ionization ML at 9.3 eV represents primarily the Mn–Si σ bond.

Correlation with Other Properties. Thus all of the results above signify that this complex has proceeded very far toward formation of a d^4 Mn^{III} center. Oxidative addition of a Si–H bond has taken place resulting in the formation of individual Mn–Si and Mn–H bonds. Structural features of this complex also point to formation of a directed Mn–Si bond. For instance, the 3-fold axis of the $SiCl_3$ ligand points within a few degrees of the metal center for formation of the Mn–Si bond. The few degrees distortion is within expectations from crowding. Also, the Mn–Si bond in this complex is only 0.03 Å longer than the Fe–Si bond in $CpFe(CO)_2SiCl_3$, which represents a complex with a normal M–$SiCl_3$ bond in the absence of the Si–H interaction.[52] The slightly longer Mn–Si bond is consistent with the greater radius of Mn in comparison to Fe. Other chemical and physical properties are also related to this bonding description, as described below.

A. Substitution Rates. The coordinated silane undergoes substitution by triphenylphosphine according to the reaction[20]

$$CpM(CO)_2HSiR_3 + PPh_3 \rightarrow CpM(CO)_2PPh_3 + HSiR_3$$

The rate of this substitution reaction provides a measure of the extent of addition of the Si–H bond to the metal center. For instance, the rate of reaction of $CpMn(CO)_2HSiPh_3$ with PPh_3 is relatively fast for this class of complexes. Other studies of this triphenylsilyl complex have shown that the Si–H bond interaction with the metal in this case is relatively weak and apparently dominated by 2-electron donation from the Si–H bond to the metal to form a three-center Mn–H–Si bond.[25,26] The substitution reaction in this case may be viewed as replacement of one 2-electron-donor ligand by another 2-electron-donor ligand. In contrast, the reaction rate of $CpRe(CO)_2HSiPh_3$ with PPh_3 is 10^6 times slower. This Re compound has directed Re–Si and Re–H bonds (Re^{III}). The distance between the Si and H atoms is 2.2 Å, which is too long to assume any significant retention of Si–H interaction.[53] This substitution reaction requires reductive elimination of the silane before replacement with the phosphine. The substitution reaction of $CpMn(CO)_2HSiCl_3$ has a rate that is more similar to that of the rhenium complex. These kinetic studies indicate that a Mn^{III} center with independent Mn–H and Mn–Si bonds is also the preferred description of the bonding in $CpMn(CO)_2HSiCl_3$.

B. Proton Abstraction. For another comparison of reactivities, proton abstraction on $CpMn(CO)_2HSiCl_3$ can be done with a weak base such as Et_3N to give $CpMn(CO)_2SiCl_3^-$. Proton abstraction from $CpMn(CO)_2HSiPh_3$ requires a stronger base such as NaH.[22] It is worth noting that reprotonation of the $CpMn(CO)_2SiCl_3^-$ anion occurs at the cis position to $SiCl_3$ to yield the same complex.[23,54] Other ligands and atoms that are more sterically demanding than hydrogen substitute trans to $SiCl_3$.[54] The substitution of the proton cis to the Si has been proposed as evidence for a stabilizing Si–H interaction that is not possible with substituents larger than H.[23] We carried out Fenske–Hall calculations on $[CpMn(CO)_2SiCl_3]^-$ to help examine the reprotonation reaction. The proton will seek the most available electron density, which is the HOMO of the anion.[55,56] The orbital description of the $[CpMn(CO)_2SiCl_3]^-$ anion is very well known from other studies of $CpMn(CO)_2L$ complexes. In these complexes, L is a 2-electron-donor ligand like $SiCl_3^-$ with poor π-acceptor ability (poorer than CO). The HOMO of the complex is basically the d_{yz} orbital, which is strongly hybridized toward the ligand L, not much different from the metal orbital shown in Figure 3. This orbital in the anion is not stabilized by π-backbonding to $SiCl_3^-$ and is most susceptible to the stabilizing interaction with the proton. The hybridization of this orbital toward the ligand side of the molecule[36] means that the protonation will be most favored cis to $SiCl_3$ rather than on the Cp side of the complex. Thus proton substitution in the cis position is favored because of the directional nature of the Mn–H interaction and does not require protonation of the Mn–Si bond or interaction with the silicon.

The bonds from the metal to $SiCl_3$ and H involve the hybrid combinations of the primarily d_{yz} and d_{z^2} orbitals. These are the HOMO and LUMO of the complex, respectively, and are the orbitals most available for forming the bonds. The hybrid bonds obtained from the Fenske-Hall calculations weigh the contribution of the d_{yz} orbital more than the d_{z^2} and yield an angle between the directed hybrids of about 65°. An equal weighing of the d_{yz} and d_{z^2} orbitals in the hybrids corresponds more closely to complete oxidative addition to form the individual directed bonds. It is interesting that the equal weighted hybrids form a bond angle of 49°, and the Si–Mn–H bond angle observed in the complex is 50–55°. Thus the directed hybrids from the metal help hold the Si and H atoms in close proximity in this complex. Substituents larger than hydrogen will be less able to access the metal hybrid in the cis position.

C. ^{29}Si NMR. One of the most widely used techniques for investigating the possibility of direct Si–H interaction in the complex is ^{29}Si NMR and the measured J_{Si-H} coupling constants.[21] The coupling constant of a normal covalent Si–H bond is typically about 200 Hz. The J_{Si-H} of $MeCpMn(CO)_2HSiCl_3$ is 54.8 Hz while that of $MeCpMn(CO)_2HSiPh_3$ is 64 Hz.[21] In contrast, the coupling constants of compounds where the silyl and hydride are

(51) Cradock, S.; Ebsworth, E. A. V.; Robertson, A. *J. Chem. Soc., Dalton Trans.* **1973**, 22–26.
(52) Schubert, U.; Kraft, G.; Walther, E. *Z. Anorg. Allg. Chem.* **1984**, *519*, 96–106.
(53) Smith, R. A.; Bennett, M. J. *Acta Crystallogr.* **1977**, *B33*, 1113–1117.
(54) Carre, F.; Colomer, E.; Corriu, R. J. P.; Vioux, A. *Organometallics* **1984**, *3*, 1272–1278.
(55) Hriljac, J. A.; Harris, S.; Shriver, D. F. *Inorg. Chem.* **1988**, *27*, 816–821.
(56) Harris, S.; Bradley, J. S. *Organometallics* **1984**, *3*, 1086–1093.

independent ligands, like $(CO)_4FeHSiPh_3$, are significantly smaller at about 20 Hz.[21] The J_{Si-H} of the $CpMn(CO)_2HSiR_3$ complexes are intermediate between that of a covalently bonded Si-H and a nonbonded Si-H. These intermediate coupling values have been cited as evidence for some amount of Si-H bonding interaction being retained in these complexes. Alternatively, calculations of NMR coupling constants have shown that nonbonding contacts between atoms that are closer than van der Waals distances will dominate the value of the coupling constant between the atoms.[57,58] The distance between the silicon and hydrogen atoms in this complex is 1.8 Å, which is shorter than the van der Waals distance of 3.1 Å for neutral atoms. We attribute the intermediate value of the coupling constant in $CpMn(CO)_2HSiCl_3$ to nonbonded NMR coupling. This coupling is a consequence of the inherently narrow angle between the d_{yz} and d_{z^2} metal hybrids, which holds the Si and H atoms in close proximity, and not to the presence of a weak bond between the Si and the H.

Conclusions

The results on this Si-H addition to the metal differ from the results of C-H interaction with the metal in (cyclohexenyl)-manganese tricarbonyl. The photoelectron information on the cyclohexenyl complex did not give measurable interaction of the C-H σ^* orbital with the metal center. The Si-H σ^* is naturally lower in energy than the C-H σ^* allowing more effective interaction of the Si-H σ^* with the filled metal orbitals. The Cl substituents on the Si also aid in this interaction because of the electronegativity of Cl. The net result is that both the σ and σ^* levels collapse in $CpMn(CO)_2HSiCl_3$ to give Mn-H and Mn-Si bonds. In (cyclohexenyl)manganese tricarbonyl, the donation of the σ C-H electrons to the empty metal LUMO's was the major interaction. In $CpMn(CO)_2HSiCl_3$, although the latter interaction is always present, the interaction of the metal HOMO with the Si-H σ^* plays a more important role.

With these two complexes we have now observed the effects of strong interaction with the metal center (the Si-H case) and weak interaction with the metal center (the C-H case). It remains to be seen if molecules in the intermediate regions of interaction can be characterized so that the crossover between the two limits can be understood. Molecules of the form $CpM(CO)(L)HSiR_3$ offer the possibility of characterizing a wide range of electron donating and accepting abilities of the metal complex and the Si-H bond. Molecules have been prepared for observing the effects of different R substituents (F, Cl, alkyl, phenyl), different ligands L (CO, PPh_3, PMe_3, CNR), different methylated cyclopentadienyls, and different metals. It appears possible to tune the extent of interaction and electron donation/acceptance between the metal and the silane. Photoelectron spectroscopy is important to characterization of the actual electron distribution and bonding in these complexes.

Acknowledgment. We acknowledge support by the U.S. Department of Energy (Division of Chemical Sciences, Office of Basic Energy Sciences, Office of Energy Research, DE-AC02-80ER 10746), the National Science Foundation (CHE8519560), the donors of the Petroleum Research Fund, administered by the American Chemical Society, and the Materials Characterization Program, Department of Chemistry, University of Arizona. We thank Swati Chattopadhyay for help in assembling figures. We also gratefully acknowledge helpful discussions with Dr. Ulrich Schubert and Dr. R. J. P. Corriu.

(57) Barfield, M.; Della, E. W.; Pigou, P. E.; Walter, S. R. *J. Am. Chem. Soc.* **1984**, *106*, 5051-5054.
(58) Barfield, M.; Della, E. W.; Pigou, P. E.; Walter, S. R. *J. Am. Chem. Soc.* **1982**, *104*, 3549-3552.

Thiolate, Thioether, and Thiol Derivatives of Iron(0) Carbonyls

Wen-Feng Liaw,[†] Christine Kim,[†] Marcetta Y. Darensbourg,*[,†] and Arnold L. Rheingold[‡]

Contribution from the Departments of Chemistry, Texas A&M University, College Station, Texas 77843, and University of Delaware, Newark, Delaware 19716. *Received July 27, 1988*

Abstract: A new series of anionic complexes of iron tetracarbonyl monofunctionalized with the ligand $[RS^-]$, $[RSFe(CO)_4^-]$ (R = Ph, Et, Me, H), have been synthesized and characterized. The compound $[PPN][PhSFe(CO)_4]$ was formed in the reaction of $[PPN][HFe(CO)_4]$ and PhSSPh. The $[PhSFe(CO)_4^-]$ anion was characterized by X-ray diffraction as its $[PPN^+]$ salt and found to be a typical trigonal-bipyramidal complex in which the phenylthiolate ligand occupies an axial position with a Fe-S bond distance of 2.332 (5) Å and ∠Fe-S-C(Ph) = 111.3 (6)°. The salt crystallized in the orthorhombic space group $Pbc2_1$, with a = 9.529 (4) Å, b = 21.493 (9) Å, c = 20.185 (9) Å, V = 4134 (3) Å^3, and Z = 2. Other members of the series of complexes, $[RSFe(CO)_4^-]$, were best obtained by ligand exchange of $[RS^-]$ and the labile thioether complex $(PhSMe)Fe(CO)_4$. The latter was produced from the low-temperature alkylation of the $[PhSFe(CO)_4^-]$. Protonation of the thiolates (R = Ph, Et, Me, H) ultimately leads to formation of H_2 and $Fe_2(\mu\text{-}SR)_2(CO)_6$; however, the intermediate thiol, $(RSH)Fe(CO)_4$, could be observed at −78 to −40 °C for R = Et, Me. The PhSH and HSH derivatives were unstable even at −78 °C.

Advances in the understanding of reaction pathways at a metal-ligand site, particularly those of hydride and hydrogen atom transfer from hydridometalcarbonyl anions,[1] have suggested analogous reactivity approaches to other $M-X^-$ functionalities. Accessible for investigation is a wide range of functionalities in the series $XM(CO)_5^-$; where M = Cr, Mo, and W and X may be H^-, all the halides, pseudohalides, carbon donor ligands, oxygen donor ligands such as O_2CR^-, OR^-, or OAr^-, and sulfur donor ligands such as SR^- or SAr^-. However, for the analogous $XFe(CO)_4^-$ complexes, X is limited to the well-known hydride derivative,[2] C donor ligands,[3] and cyanide.[4] Derivatives of anionic oxygen donor ligands are unknown as are all halides with the possible exception of iodide.[5] Simple thiolate derivatives had been proposed as intermediates in reactions of thioketones with $HFe(CO)_4^-$, prepared in situ from $Fe(CO)_5$ and KOH;[6] however, there

[†] Texas A&M University.
[‡] University of Delaware.

(1) Darensbourg, M. Y.; Ash, C. E. *Adv. Organomet. Chem.* **1987**, *27*, 19
(2) Smith, M. B.; Bau, R. *J. Am. Chem. Soc.* **1973**, *95*, 2388.
(3) Gartzke, W.; Huttner, G. *Chem. Ber.* **1975**, *108*, 1373.
(4) Goldfield, S. A.; Raymond, K. N. *Inorg. Chem.* **1974**, *13*, 770.
(5) Abel, E. W.; Butler, I. S.; Jenkins, C. R. *J. Organomet. Chem.* **1967**, *8*, 382.

0002-7863/89/1511-3591$01.50/0